provides support for the continued investigation of this regimen for the initial treatment of GBM.

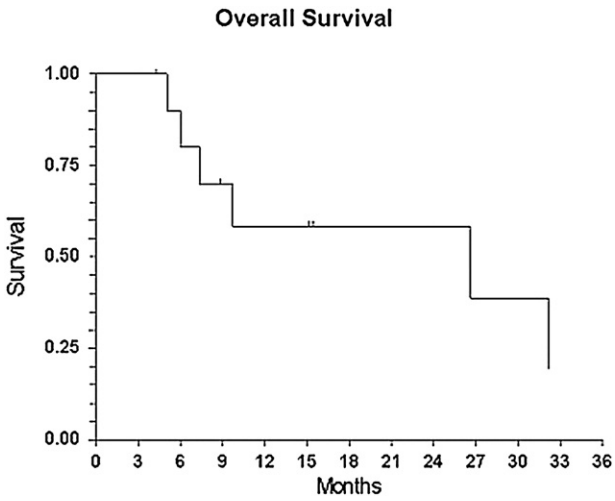

POSTER DISCUSSION III: PROSTATE
Saturday May 1, 2010
7:30 AM–8:45 AM

PD36

High-Dose-Rate Re-Irradiation with Continuous Hyperthermia for Recurrent Prostate Cancer

Nasiruddin Mohammed, M.D., M.B.A., Michel I. Ghilezan, M.D., Ph.D., Larry Kestin, M.D., Peter Chen, M.D., Hong Ye, M.S., Frank A. Vicini, M.D., Alvaro A. Martinez, M.D. Radiation Oncology, William Beaumont Hospital, Royal Oak, MI.

Purpose: To report our institutional experience using hyperthermia and high-dose-rate brachytherapy (HyT+HDR) for the treatment of locally recurrent prostate cancer after previous irradiation.
Materials and Methods: Since 2001, we have employed a protocol using HyT+HDR for previously irradiated patients with biopsy proven recurrent prostate cancer. Prior to treatment, patients underwent restaging including PSA, bone scan, and pelvic MRI or CT to rule out metastatic disease. HDR technique was similar to our previously published experience. Optimal needle positions were generated intraoperatively using an on-line interactive software program. Real-time dosimetry was employed to provide conformal coverage of the gland. Treatment was delivered to a dose of 28 Gy in four fractions of 7 Gy each with a minimal interfraction time of 6 hours. All patients had six interstitial thermometers placed into the prostate gland at various positions. Each thermometer provided 4 points of measurement along its length for a total of 24 points of thermometry within the prostate gland and surrounding tissues. Continuous, steady-state interstitial heating was achieved to a target temperature of 41 − 42 ^{o}C via an in-house customized template system for 18 hrs/day with minimum of 3 hrs of heating prior to each fraction of RT. Patients were followed with regular PSA and DRE for development of biochemical failure (BF = nadir+2) or a clinical event (CE = initiation of androgen ablation (AA), locoregional recurrence, or distant metastasis (DM)). Various treatment parameters along with initial and recurrent disease characteristics were assessed for correlation with clinical outcome and toxicity after continuous low temperature HyT+HDR.
Results: A total of 10 patients have been re-irradiated at our institution using HyT+HDR between 2/2001 and 8/2009 with a median followup of 28 mo. Median initial Gleason score was 6 (4-7), median max recurrence PSA prior to retreatment was 5.4 ng/mL (2.9-15 ng/mL). All patients were either clinical stage II or III at initial presentation with the exception of one patient who was pT3a after radical prostatectomy and received adjuvant radiation. Median initial external beam radiation dose was 66.6 Gy (64.8–75.6 Gy) and one patient received an ^{125}I implant with a planned dose of 144 Gy. The median time to initial BF post initial RT was 50 mo and the median time from failure to HyT+HDR was 16.6 mo. A CE after HyT+HDR occurred in 5 patients after a median of 23.3 mo despite 60% of all patients achieving PSA nadir of $\leqslant$ 0.1 ng/mL. AA was initiated in all five of these patients due to rising PSA with one patient ultimately developing distant metastasis at 19 mo and dying at 32 mo post re-irradiation. BF occurred in 6 patients at median of 21 mo post re-irradiation. The two year rates of BC and freedom from CE were 44% and 60% respectively. Max acute (<90 days) or chronic GU toxicity $\geqslant$ grade 3 was seen in 2 patients. Max acute or chronic GI toxicity $\geqslant$ grade 3 was not seen. No tumor, patient, or treatment related characteristics correlated significantly with BF, CE, or toxicity.
Conclusions: HyT+HDR for salvage after previous irradiation appears to be a tolerable treatment that can offer cure in a proportion of higher risk salvage patients with acceptable toxicity. Continued followup and additional patients are necessary to identify factors associated with toxicity and outcome.

PD37

Simulation of Needle Insertion and Tissue Deformation for Modeling Prostate Brachytherapy

Nuttapong Chentanez, M.S.[1], Ron Alterovitz, Ph.D.[3], Daniel Ritchie[1], Lita Cho, B.S.[1], Kris K. Hauser, Ph.D.[4], Ken Goldberg, Ph.D.[2], Jonathan R. Shewchuk, Ph.D.[1], James F. O'Brien, Ph.D.[1] [1]Electrical Engineering and Computer Sciences, University of California, Berkeley, Berkeley, CA; [2]Industrial Engineering and Operations Research, University of California, Berkeley, Berkeley, CA; [3]Computer Science, University of North Carolina at Chapel Hill, Chapel Hill, NC; [4]School of Informatics and Computing, Indiana University at Bloomington, Bloomington, IN.

Purpose: Realistic modeling of needle insertion during Brachytherapy can be used for training and in automated planning to reduce errors between intended and actual placement of the needle tip. We have developed a 3D tetrahedral finite element simulation that models tissue deformation, needle flexation, and their coupled interaction. This system addresses the following applications:

- Training physicians to compensate for tissue deformation during needle insertion.
- Incorporating a model of tissue deformation into manual and automated planning for seed placement and dose distribution.
- Developing automated steering procedures for robotic devices.

Materials and Methods: We model tissue elasticity with constitutive equations discretized over a 3D tetrahedral mesh by a finite element method. The needle is modeled as a stiff elastic rod. The two systems are coupled together by shared nodes, and the tissue and needle are dynamically remeshed to allow needle insertion and withdrawal. Nodes are dynamically positioned along a curvilinear needle path in a volumetric mesh, enabling the simulation to apply accurate cutting and frictional forces along the needle shaft and at the needle tip.
Results: We can realistically and interactively simulate needle insertion on a high-resolution prostate mesh at 25 frames per second on an 8-core 3.0 GHz PC. External mesh boundaries conform to the skin, and internal faces conform to organ boundaries, separating regions with dissimilar material properties. The code can model both rigid and flexible needles. Figure 1.a shows a screenshot from the simulator running the prostate brachytherapy scenario. The inset image shows a cutaway view of the finite element mesh used by the simulation. To evaluate the accuracy of the simulation we compare against experiments in which flexible, nitinol needles of diameter 0.83 mm were robotically inserted into a gel tissue phantom. Video showing the needle and motion of fiducial markers was recorded. We then simulated the same configuration and compared the recorded and simulated markers. Figure 1.b shows the simulated needle in yellow and simulated fiducials in white superimposed over the recorded video. The needle trajectories match to within video resolution, and the

root-mean-squared error of the marker positions over time is 0.75 mm, with 88.3% of errors under 1 mm and 97.8% of errors under 2 mm.

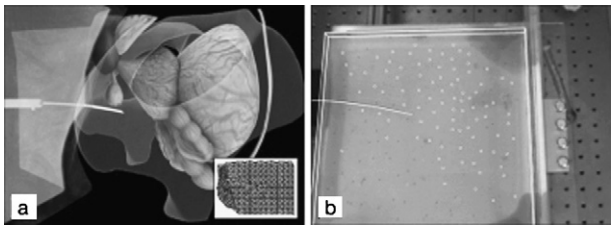

Conclusions: Our key technical contributions include a fast local remeshing method, an efficient algorithm for computing the coupling forces between tissue and needle, and optimizations to allow realtime performance for high-resolution models. A detail description of the simulation code with example videos is posted at www.cs.berkeley.edu/b-cam/Papers/Chentanez-2009-ISN. This simulation can be used as a training tool to help physicians anticipate and compensate for placement errors due to tissue deformation. We are also exploring applications in automated planning and robotic insertion.

PD38

What Is the Optimal Dose for Real-Time Prostate Brachytherapy? The Use of ESTRO/EAU/EORTC 2007 Volume Definitions to Achieve a Post Implant D90 >140 Gy

Nicola L. Dallas, FRCR.[1], Andrew J. Doggart, M.Sc.[1], Joanne C. Jones, M.Sc.[1], Peter R. Malone, M.S.[2], Adam Jones, M.D.[2], Paul B. Rogers, FRCR.[1] [1]Berkshire Cancer Centre, Royal Berkshire Hospital, Reading, Berkshire, United Kingdom; [2]Harold Hopkins Department of Urology, Royal Berkshire Hospital, Reading, Berkshire, United Kingdom.

Purpose: A minimum D90 of 140 Gy to the prostate has been shown by Stock and Stone to result in superior freedom from biochemical failure. To date there is no recommended real-time intraoperative D90 specified to achieve this. We analyzed the intraoperative and post implant dosimetry (PID) using the ESTRO/EAU/EORTC 2007 recommendations and report our experience of the D90, V100, V150, V200 to the prostate (CTV-P) and the D90 to the prostate margin (CTV-PM) to see what intraoperative CTV-P dose would achieve 140 Gy post implant. Analysis of PID urethral D30 and rectal V100 and the rectal bleeding, recatheterization and urethral stricture rates was used to define the tolerability of this dose.
Materials and Methods: 181 men with early prostate cancer were treated with transperineal interstitial low-dose-rate brachytherapy (BT), using the real-time intraoperative ProSeed technique, between November 2003 and June 2008. Median followup was 30 months (12-60). Patients were stratified by risk. Low-risk disease (T1-2, Gleason 6, PSA<10) received BT alone. Intermediate risk disease (T1-2, Gleason 7, PSA 10-20) received BT and 6 months anti-androgen therapy. The intended dose was 160 Gy to the CTV-PM; the Variseed software calculates the dose to the CTV-P in real-time providing a CTV-PM calculation once the procedure is complete. 175 (97%) patients had a PID CT scan after 4 weeks. The CTV-PM is the prostate with a 3-dimensional volume expansion of 3mm constrained to 0mm posteriorly to the rectal wall, and cranially to the bladder. These data were available for 166 patients (92%). Biochemical disease relapse was defined using both the ASTRO 1997 and ASTRO Phoenix 2005 consensus definitions.
Results: The mean intraoperative D90 to the CTV-P was 188 Gy (163-215 Gy) falling to 175 Gy (138-222 Gy) on the PID scan. The mean intraoperative CTV-P V100 was 99% (91-100%), falling to 94% (74-100%) at PID. The mean CTV-P V150 was 50% (22-72%) and 53% (31-83%) at implant and post-implant, respectively. The mean CTV-P V200 was 20% (8-32%) at implant rising to 24% (9-60%) post implant. The mean CTV-PM D90 was 165 Gy (154-177 Gy) intraoperatively and 148 Gy (116-183 Gy) on PID. 98.9% (173 patients) received a PID D90 ⩾140 Gy to the CTV-P. The PSA relapse rate was 2.3% (4 patients) using both definitions. Only 2 patients received <140 Gy to the post implant CTV-P, neither relapsed biochemically. The mean PID urethral D30 was 197 Gy (103-346 Gy). The recatheterization rate was 2.2% and the urethral stricture rate was 1.7%. The mean PID rectal V100 was 1.04 cc (0.06-3.84cc). 4.4% patients reported mild rectal bleeding. There were no rectovesical fistulas.
Conclusions: The use of the ESTRO/EAU/EORTC 2007 volume definitions is important in establishing consistent reporting enabling meaningful comparison between brachytherapy techniques and centers. Following this study, we would recommend an intraoperative D90 to the CTV-P of 185 Gy. By doing this the intraoperative CTV-PM D90 of 160 Gy was achieved which gave a post implant D90 ⩾140 Gy to the CTV-P in 98.9% patients. The low relapse rate in this group acknowledges the importance of the 140 Gy D90 to the PID CTV-P as a quality standard. This dose is well tolerated as evidenced by the low rectal bleeding, recatheterisation and urethral stricture rates observed.

PD39

Optimal Reconstruction Method for Intraoperative Seed Localization Using Fluoroscopy in Prostate Brachytherapy

Junghoon Lee, Ph.D.[1], Danny Y. Song, M.D.[1], Everette C. Burdette, Ph.D.[2], Gabor Fichtinger, Ph.D.[3], Jerry L. Prince, Ph.D.[1] [1]Radiation Oncology, Johns Hopkins University, Baltimore, MD; [2]Acoustic MedSystems, Champaign, IL; [3]School of Computing, Queen's University, Kingston, ON, Canada.

Purpose: The ability to intraoperatively localize the implanted seeds during permanent prostate brachytherapy will provide an immediate indication of dosimetric quality of implantation. Our purpose was to design and validate a novel seed reconstruction method that is able to accurately determine the implanted seed positions from three or more X-ray fluoroscopy images within near-real-time.
Materials and Methods: The seed reconstruction problem is formulated as a combinatorial optimization problem and solved by a reduced-dimensionality seed-matching algorithm (REDMAPS). REDMAPS takes the geometry of the cone-beam backprojection into account and makes a significant amount of dimensionality reduction (>97%) of the original problem possible. The reduced problem is solved using linear programming in under 10 seconds. Three X-rays are acquired for reconstruction using non-isocentric C-arm fluoroscopy, and a non-invasive fluoroscope tracking fiducial is used for registration of the reconstructed 3D seed coordinates to the ultrasound frame as well as computation of the C-arm pose. Intraoperative dosimetry using REDMAPS requires only modest alterations to a standard brachytherapy setup by separately computing the 3D seed positions using mobile C-arm and transferring the calculated positions into the treatment planning software for visualizing the dose distribution intraoperatively. Seed localization accuracy of REDMAPS in terms of seed detection rate and localization error under various imaging conditions was assessed on simulations and 5 phantoms. REDMAPS was also validated on 21 patient datasets acquired from 8 patients with palladium seeds.
Results: In simulations, REDMAPS identified over 99% of the seeds with a localization error less than 0.5mm when the C-arm is calibrated and the poses are known with no errors. Under realistic calibration and pose errors, it still achieved seed detection rate over 98% and localization error less than 0.5mm. For phantom and clinical datasets, overall seed detection rate was over 98% and the mean reconstruction (or projection) error was less than 1mm. Although REDMAPS is formulated for any number of images, it could achieve this clinically excellent seed detection and localization accuracy by using only three images. Since total computation time for reconstruction was less than 10 seconds in most cases, it does not interfere with the clinical workflow with respect to any OR delays.
Conclusions: Utilizing a conventional non-isocentric C-arm fluoroscope, REDMAPS is sufficiently accurate, robust, and computationally efficient to enable intraoperative seed reconstruction with minimum alteration of clinical workflow. This provides a software solution not requiring specialized hardware, using only existing equipment in the OR for intraoperative dynamic dosimetry.